A comparative investigation of lithium(I) biosorption properties of *Aspergillus versicolor* and *Kluyveromyces marxianus*

Hande Günan Yücel, Zümriye Aksu, Gülşah Büşra Yalçınkaya, Sevgi Ertuğrul Karatay and Gönül Dönmez

ABSTRACT

In the current batch study, lithium(I) ion sorption behaviors of *Aspergillus versicolor* fungus and newly isolated *Kluyveromyces marxianus* yeast were investigated comparatively. Surface and structural characterization studies of the biosorbents carried out with Fourier transform infrared spectrometer (FTIR), scanning electron microscope (SEM), surface area and zeta potential analyses showed that isolated *K. marxianus* yeast from salty wastes has more preferable properties (i.e. higher porosity, surface area and negativity) for cation sorption. Biosorption studies also supported this estimation; higher lithium(I) sorption capacities were obtained with *K. marxianus* cells at all experimental conditions studied. Rapid sorption profiles of the sorbents demonstrated that physical interaction is the main mechanism in this system. The effects of pH and initial lithium(I) concentration on the lithium(I) sorption capacities of biosorbents were examined. The maximum adsorption capacities of 347.9 and 409.2 μmol lithium(I)/g biosorbent were obtained at an initial lithium(I) concentration of 20 mg/L at pH 9.0 using *A. versicolor* and *K. marxianus*, respectively. The equilibrium data fitted both Langmuir and Freundlich models in the concentration ranges studied. This study revealed that *K. marxianus* yeast can be used for effective, rapid and low cost capture process of lithium(I) ions from aqueous solutions.

Key words | *Aspergillus versicolor*, biosorption, fungus, *Kluyveromyces marxianus* yeast, lithium(I) ion

Hande Günan Yücel
Zümriye Aksu
Chemical Engineering Department,
Hacettepe University,
06800, Ankara,
Turkey

Gülşah Büşra Yalçınkaya
Sevgi Ertuğrul Karatay (corresponding author)
Gönül Dönmez
Biology Department, Science Faculty,
Ankara University,
06100, Ankara,
Turkey
E-mail: *sertugrul@ankara.edu.tr*

INTRODUCTION

Lithium, which is the lightest metal in the world, plays critical roles in different industries due to its characteristic properties such as low melting point, low density and high heat capacity (Jeppson *et al.* 1978). Since its specific physical and chemical properties provide important advantages, it finds usage in various applications like lithium-ion batteries, pharmaceuticals, ceramics, light aircraft alloys and as a tracer in wetlands (Headley *et al.* 2005; An *et al.* 2012; Bodin *et al.* 2012; Park *et al.* 2012). In addition to rapid expansion in the electric vehicles market, the extensive demand for rechargeable batteries and future aspects for their usage in energy storage systems lead to the necessity of the recovery of lithium from its limited resources with high efficiency and low cost (Park *et al.* 2012; Kim *et al.* 2015). A great majority of the lithium is found within the rocks called 'pegmatites' and the brines. The process of ionic lithium recovery from brines and seawater is more preferable than chemically bonded lithium recovery from pegmatites (Peiro *et al.* 2013).

Various lithium separation methods from aqueous solutions like filtration, extraction, precipitation and ion exchange were developed; but adsorption is known to be the most advantageous one (Chitrakar *et al.* 2001; Bi *et al.* 2014). Nevertheless, there is limited information on lithium recovery by using biological methods, i.e. bioaccumulation and biosorption, which would be cost effective and eco-friendly if the process is carried out at optimum conditions. For lithium(I) ion recovery from aqueous solutions, biosorption would be a good alternative since the process is rapid and enables lithium(I) ion interaction with the functional groups such as carboxyl, hydroxyl, phosphate and sulphate. In addition, using non-living cells in dried form is expected

doi: 10.2166/wst.2020.126

to be more efficient due to non-dependence of growth media components, convenience in stocking, easiness of desorption and higher surface affinity (Arıca *et al.* 2005; Nath & Ray 2015).

Despite the mentioned advantages of using microorganisms, there are few studies in the literature on biosorption of lithium from aqueous solutions. Lithium sorption capacities of various microorganisms were tested at a specified condition by Tsuruta (2005). It was stated in the study that biosorption capacities of the cells varied due to cell wall structures of the microbial strains. Alternatively, a study on lithium biosorption using a biofilm matrix was presented by Kurniawan & Yamamoto (2015). Our previous study also showed that the new biomass-based hybrid adsorbent prepared from *Pichia stipitis* yeast displayed significantly greater lithium sorption capacity than the untreated cells (Günan-Yücel & Aksu 2019). In all studies, lithium biosorption took place rapidly with mainly physical interaction.

This is the first comparative and detailed study in the literature that investigating lithium(I) ion biosorption characteristics of *Aspergillus versicolor*, which removed effectively textile dyes at different chemical structures and different heavy metals in our previous report (Taştan *et al.* 2010), and *Kluyveromyces marxianus* isolated from salty food wastes, which has high capability for removing textile dyes (unpublished data). For this purpose, surface and structural characterization of the cells were carried out first. Next, effects of the parameters on biosorption characteristics of the cells were investigated and compatibility of the experimental data with the equilibrium isotherms was tested. Because of the limited information about lithium(I) ion biosorption, the data obtained from the current study contributes to the literature.

MATERIALS AND METHODS

Cultivation of biomass

The microorganisms were cultivated in molasses media in the current study. The composition of the growth medium was molasses solution, 1.0 g/L $(NH_4)_2SO_4$, and 0.5 g/L KH_2PO_4 (Aksu & Dönmez 2000). The pH of the growth medium was adjusted to 5.0 with 0.01 M sulfuric acid or 1 M sodium hydroxide solution. Once inoculated, 250 mL Erlenmeyer flasks containing 100 mL of sterile medium were incubated on an orbital shaker at 100 rpm at 30 °C for 5 days for *A. versicolor* and 3 days for *K. marxianus*, respectively. As the highest biomass concentrations were obtained, these incubation times were selected for the cultivation of tested microorganisms.

Preparation of biosorbent

After the growth period, the fungal biomass was filtered with Whatman Paper and then dried at 60 °C for 24 h while yeast cells were centrifuged at 5,000 rpm and the pellet was dried at 60 °C for 12 h. Our previous study showed greater performance of the dried cells since their surface affinity is higher. In addition, the water shell around the lithium ion due to its strong hydration in water is an obstacle for its interaction with the ligands found on the sorbent surface and using dried cells provided significant advantage on biosorbent–lithium interaction (Mähler & Persson 2012; Nath & Ray 2015; Günan-Yücel & Aksu 2019). So, biosorbents were used in dried form by considering both the parameters of process efficiency and ease of use. For the biosorption studies, a weighed amount of dried biomass was suspended in 100 mL of double-distilled water and homogenized in a homogenizer (Janke and Kunkel, IKA-Labortechnick, Ultra Turrax T25, Germany) at 5,000 rpm for 2 min and then stored in the refrigerator. At the beginning of biosorption studies, 10 mL dried biomass suspension was contacted with 90 mL of solution containing a known concentration of lithium(I) in an Erlenmeyer flask at a defined pH value. All the final solutions contained 1.0 g/L of biosorbent.

Lithium(I) ion biosorption

The lithium(I) ion biosorption experiments were conducted in a batch system to investigate the effects of pH, initial lithium(I) concentration on lithium(I) capture capacities of the biosorbents. Experiments were employed with 1 g/L cell dosage in 150-mL flasks containing 50 mL of lithium(I) solution prepared by dilution of a 100 mg/L stock solution of LiCl (Merck) in a range of 2.5–20 mg/L. pH adjustment of the solutions were carried out before the experiments by dropwise addition of dilute HNO_3 and NaOH solutions. The flasks were stirred at a fixed speed (100 rpm) and temperature (25 °C) in a rotary shaker for 24 h.

The lithium(I) ion biosorption capacities of the biosorbents at any time (q, mg/g) were calculated as follows:

$$q = \frac{C_o - C}{X} \quad (1)$$

where C_o is initial lithium(I) concentration (mg/L), C is the lithium(I) concentration at any time (mg/L), and X is the biosorbent concentration (g/L).

The lithium(I) biosorption percentage was defined as follows:

$$\%\ \text{Adsorbed amount of lithium(I)} = \frac{C_o - C_e}{C_o} \times 100 \quad (2)$$

where C_e is the equilibrium lithium(I) concentration (mg/L).

Equilibrium isotherms

Adsorption equilibrium studies are required to predict adsorption behavior of the adsorbent by describing the interaction between adsorbent and adsorbate (Aksu & Dönmez 2006). In this study, convenience of equilibrium data to the Langmuir and Freundlich isotherm models, which are indicated as the most preferred models due to obeying to the experimental data with high accuracy in the great majority of the academic studies, were evaluated (Beni & Esmaeili 2020). In this context, the equilibrium data were investigated for lithium(I) sorption on the biosorbents from aqueous solutions containing lithium(I) ions in concentrations in the range of 2.5–20 mg/L at 25 °C and initial pH of 9.

Langmuir isotherm

The Langmuir isotherm model is based on monolayer adsorption onto a homogeneous surface i.e. identical active sites show equal affinity to the adsorbate (Crini *et al.* 2007; Farooq *et al.* 2010). It is expressed as:

$$q_e = \frac{q_{max} K_L C_e}{1 + K_L C_e} \quad (3)$$

where q_e is the amount of lithium(I) adsorbed at equilibrium (mg/g), q_{max} is the maximum adsorption capacity of the adsorbents (mg/g), and K_L is the Langmuir isotherm constant related to the binding energy (L/mg) (Crini *et al.* 2007).

Freundlich isotherm

The Freundlich isotherm model assumes that a non-ideal multilayer adsorption process occurs on heterogeneous surfaces and adsorbate molecules interact with each other (Negm *et al.* 2018). It is represented as follows:

$$q_e = K_F C_e^{1/n_F} \quad (4)$$

where K_F is the Freundlich constant attributed to the adsorption capacity $(mg/g)(L/mg)^{1/nF}$, and n_F represents adsorption strength on the sorbent. The n_F value which is higher than 1 indicates that adsorption is a favorable and relatively strong process (Negm *et al.* 2018).

Analytical methods

Lithium(I) concentration of the samples were determined by using atomic absorption spectrometer (AAS) (Thermo Scientific iCE 3000 Series, USA). Surface functional groups of the biosorbents were analyzed with a Fourier transform infrared spectrometer (FTIR) (Thermo Scientific Nicolet 6700 Smart iTR, USA). The morphological properties of the biosorbents were characterized using a scanning electron microscope (SEM) (ZEISS Evo-50, Germany). Image processing program ImageJ was used to make the dimension calculations. Specific surface area and pore dimensions of the biosorbents were determined with surface area and pore size analyzer (TriStar II Plus, USA).

Statistical studies

All experiments were performed at least three times and the obtained results were presented as mean ± SD. The data were deemed to be statistically significant if standard deviations were within ±5%.

RESULTS AND DISCUSSION

Biosorbent characterization

FTIR

Metal ion biosorption is essentially a physisorption (i.e. electrostatic attraction or van der Waals interaction) or ion exchange process. So, the surface functional groups found in the biomass cell wall play a key role in metal–surface interaction and overall biosorption capacity (Pradhan *et al.* 2019). FTIR is a sensitive and rapid technique which enables to characterize biological molecules by enabling to determine the functional group contribution (Garip *et al.* 2009). Hence, it was applied to investigate cell wall structures of two fungal strains comparatively in this study. Obtained FTIR spectra for *A. versicolor* and *K. marxianus* were presented in Figure 1.

Similar spectral characteristics were observed due to similar structures of fungal cell wall compositions with some species-specific diversities. The broad bands between 3,200 and 3,500 cm^{-1} lead to the intermolecular hydrogen bonds in the OH group. The peaks appearing between

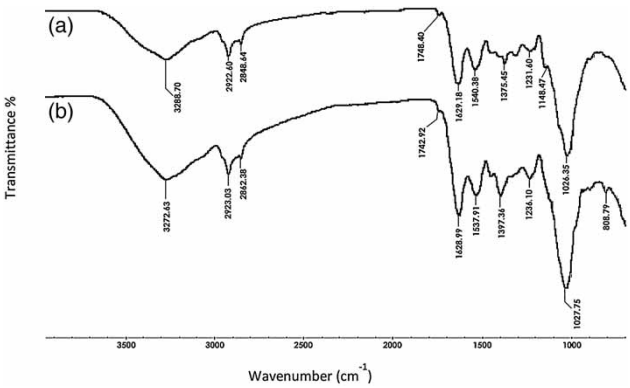

Figure 1 | FTIR spectra of (a) *A. versicolor*, (b) *K. marxianus* cells.

2,850 and 3,000 cm^{-1} show the existence of –CH bonds in amino acids and aliphatic acids present in the cell membrane. The peaks observed at 1,748 cm^{-1} and 1,742 cm^{-1} reveal the stretching vibration of C=O in ester groups found in lipid structures. The peaks appearing between 1,500 and 1,670 cm^{-1} are related to the presence of carboxylic groups in the cell wall structure (Burattini *et al.* 2008; Gohari *et al.* 2013; Shapaval *et al.* 2014). The peaks in the range of 1,355 cm^{-1} and 1,395 cm^{-1} represent the C=O bonds of COO^- symmetric stretching vibrations present in protein structures and wagging vibrations of CH_2 found in lipids and β(1–3) glucans (Potocki *et al.* 2019). The peaks between 1,220 cm^{-1} and 1,240 cm^{-1} confirm the existence of PO^{2-} asymmetric stretching vibrations in DNA, RNA and phospholipids, C–O stretching vibration and O–H in alcohols at structures of the biosorbents (Kuligowski *et al.* 2012). The small peak found at 1,148 cm^{-1} at *A. versicolor* is related to C-O and C-OH carbohydrates and β(1–3) glucans. The sharp peaks observed at 1,026 cm^{-1}1 and 1,027 cm^{-1} exhibit the presence of β 1,4 glucans and the stretching of O–P–O and C–O–P bonds at both *A. versicolor* and *K. marxianus* cell wall (Zimkus *et al.* 2013; Potocki *et al.* 2019). The small peak seen at *K. marxianus* structure at 808 cm^{-1} can be explained by the existence of mannans (Burattini *et al.* 2008; Gohari *et al.* 2013). It has been reported that presence of the polar or charged groups such as carboxyl, hydroxyl and phosphates in the cell wall structure play significant roles in higher surface negativity (Bahafid *et al.* 2017). However, lithium is known to show the strongest affinity to the carboxyl group among these (Hui *et al.* 2016).

SEM

SEM images demonstrating surface morphologies of the dried and milled *A. versicolor* and *K. marxianus* cells show their irregular, raptured and heterogenous structures clearly (Figure 2). Although they have similar physical forms, the *K. marxianus* cell wall seems to have some more porous structure which is thought to influence its cation binding capacity positively.

Surface area

Volume, diameter and specific surface area values of the pores in the biosorbents were measured using nitrogen

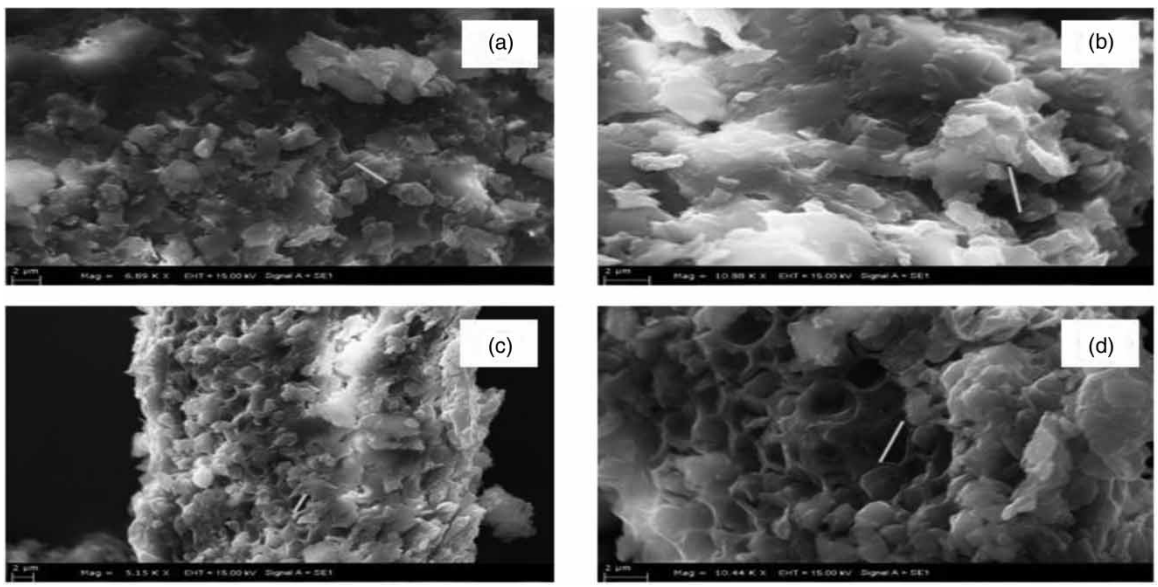

Figure 2 | SEM images of (a), (b) *A. versicolor* cells, (c), (d) *K. marxianus* cells (yellow lines refer to 3 μm). Please refer to the online version of this paper to see this figure in color: http://dx.doi.org/10.2166/wst.2020.126.

Table 1 | Surface characteristics of the biosorbents

Sample	BET surface area (m^2/g)	Total pore volume (cm^3/g)	Adsorption average pore diameter (Å)	Mean zeta potential at pH 9 (mV)
A. versicolor	1.66	0.0034	83.52	−20.28 ± 1.0
K. marxianus	3.84	0.0090	94.20	−24.55 ± 1.2

adsorption–desorption process. As it can be seen from Table 1, both surface area and pore diameter of *K. marxianus* cells are higher than those of *A. versicolor* cells, which is thought to have significant role on increasing its lithium(I) adsorption capacity.

Zeta potential

The measured mean zeta potential values of the biosorbents at the adsorption pH were tabulated at Table 1. The obtained results reveal that, higher mean zeta potential value of *K. marxianus* cells such as −24.55 mV has a clearly positive effect on sorption capacity by enhancing surface–lithium(I) physical interaction.

Biosorption experiments

Lithium(I) sorption profiles of the biosorbents were investigated for 24 h-experiments to observe the effect of contact time. However, equilibrium was reached within 5 min in all cases. Completion of the process in a short contact time seems to be quite preferable for large scale applications. This rapid biosorption trend of lithium(I) ion was also reported by Tsuruta (2005), which demonstrates the main mechanism is physisorption due to the very low molecular mass and high hydrated radius of the lithium(I) ion (Tsuruta 2005).

Effect of initial pH

Solution pH plays a critical role on metal ion adsorption capacities of the sorbents due to its direct effect on the surface charge of the biosorbent and diffusion rate of solute. In addition, during the lithium sorption process, hydrogen ion concentration is one of the most critical parameters since its competition between lithium(I) ion for binding active sites on the sorbent surface plays a key role on the lithium(I) sorption yield. In this study, pH effects on lithium(I) sorption capacities of the biosorbents were tested in the range of 3.0–10.0 (Figure 3 and Table 2). According to the experimental data, optimum pH was determined as 9 for both biosorbents, demonstrating the enhancement in lithium

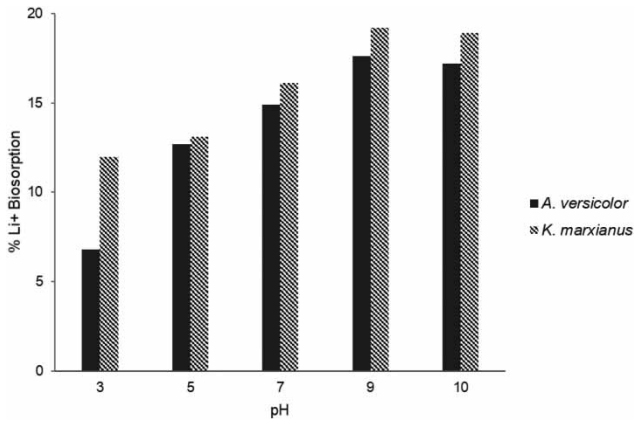

Figure 3 | Lithium(I) biosorption percentages of *A. versicolor* and *K. marxianus* at various initial pH values.

sorption capacity due to increase in available negative charged binding sites responsible for the lithium(I) sorption and decrease in protonation. The highest lithium(I) biosorption percentages and capacities were determined as 17.6%, 0.954 mg/g (137.4 μmol/g) and 19.2%, 1.069 mg/g (154.0 μmol/g) for *A. versicolor* and *K. marxianus* cells at pH 9, respectively. *K. marxianus* displayed distinctly greater performance on lithium sorption since its higher surface negativity due to the small differences in the cell wall structure enables more effective electrostatic interaction with lithium(I) ion. Increase in cation sorption capacities of various dead microorganisms at higher pH values due to strong interaction between positively charged ions and negatively charged functional groups on the biosorbent surface were presented at numerous studies (Selatnia *et al.* 2004; Sahmoune *et al.* 2009; Sahmoune 2018).

Effect of initial lithium(I) concentration

Initial lithium(I) concentration is one of the key parameters since its biosorption is a diffusion-limited physical process taking place between two phases. The influence of the initial lithium(I) concentration on maximum adsorption capacities of the biosorbents were demonstrated in Table 2. Increase in initial lithium(I) concentration resulted in enhancement in the capacities due to increasing driving force to overcome

Table 2 | Effects of biosorption parameters on lithium(I) sorption capacities of *A. versicolor* and *K. marxianus* cells

Parameter tested	Biosorbent	Initial pH	Initial Li^+ concentration (mg/L)	Biosorbent concentration (g/L)	q_m (mg Li^+/g biosorbent)	q_m (μmol Li^+/g biosorbent)	Li^+ adsorption yield (%)
Initial pH	*A. versicolor*	3	5.0	1.0	0.330 ± 0.014	47.5 ± 2.0	6.8 ± 0.3
		5			0.605 ± 0.011	87.2 ± 1.6	12.7 ± 0.2
		7			0.712 ± 0.018	102.6 ± 2.6	14.9 ± 0.4
		9			0.954 ± 0.019	137.4 ± 2.7	17.6 ± 0.3
		10			0.936 ± 0.015	134.8 ± 2.2	17.2 ± 0.3
	K. marxianus	3			0.418 ± 0.011	60.2 ± 1.6	12.0 ± 0.3
		5			0.660 ± 0.010	95.1 ± 1.5	13.1 ± 0.2
		7			0.885 ± 0.014	127.5 ± 2.0	16.1 ± 0.3
		9			1.069 ± 0.012	154.0 ± 1.7	19.2 ± 0.2
		10			1.055 ± 0.012	152.0 ± 1.7	18.9 ± 0.2
Initial Li^+ concentration	*A. versicolor*	9	2.5	1.0	0.573 ± 0.013	82.5 ± 1.9	17.4 ± 0.4
			5.0		0.954 ± 0.019	137.4 ± 2.7	17.6 ± 0.3
			10.0		1.660 ± 0.035	239.1 ± 5.0	13.5 ± 0.2
			20.0		2.415 ± 0.056	347.9 ± 8.0	10.9 ± 0.1
	K. marxianus		2.5	1.0	0.713 ± 0.012	102.7 ± 1.7	21.7 ± 0.4
			5.0		1.069 ± 0.012	154.0 ± 1.7	19.2 ± 0.2
			10.0		2.020 ± 0.031	291.0 ± 4.5	16.2 ± 0.1
			20.0		2.840 ± 0.049	409.2 ± 7.1	12.8 ± 0.1

the mass transfer limitations between solid and aqueous phases; however, adsorbed lithium(I) percentage reduced as coherent with the literature, because of the rapidly held active sites of the biosorbent surfaces (Mameri *et al.* 1999; Chergui *et al.* 2007; Sahmoune 2018). The lowest adsorption yields and the highest adsorption capacities were observed in the presence of 20 mg/L ion concentration such as 10.9%, 12.8% and 347.9, 409.2 μmol lithium(I)/g biosorbent for *A. versicolor* and *K. marxianus*, respectively.

Structural and surface analyses of the biosorbents demonstrated the significant relationship between the sorbent characteristics and their sorption capacities comparatively. FTIR spectra of the biosorbents showed the similar composition of their surfaces. The difference in surface negativities was explained with the small variations in their IR spectra. While SEM images showed their heterogeneous surfaces and little porous structure, Brunauer–Emmett–Teller (BET) results indicating their low surface area and porosity values confirmed the SEM results. Although the surface characterization of the sorbents showed their similar structures, superior surface area and zeta potential values of *K. marxianus* strain outmaneuvered it for lithium(I) sorption. The similar biosorption profiles of both strains showed that biosorption mechanisms were similar. Equilibrium was reached very rapidly in a few minutes for all cases. The maximum yields were obtained at pH 9 for both strains, at which negative surface charge density was quite high, and lithium-surface interaction was more efficient. In addition, higher surface negativity of the *K. marxianus* strain ensured higher lithium sorption capacity. These results demonstrated that main lithium sorption mechanism is a physisorption process taking place due to physical interaction with the sorbent surface. This is a reversible process and almost complete recovery of the adsorbed lithium can be carried out at acidic media (Wang & Chen 2009; Günan-Yücel & Aksu 2019).

Table 3 includes comparison of the obtained results in this study with the other reports presented in the literature. Tsuruta (2005) attained maximum biosorption capacity using Arthrobacter nicotianae bacteria from among various types of microorganisms; while effective lithium(I) biosorption was not observed onto any of the fungi strains tested. Besides, effectiveness of the *K. marxianus* yeast was stated to be significantly low in the mentioned study. However, *A. versicolor* and *K. marxianus*, which cultivated in molasses media, showed distinctly high performance on lithium(I) ion sorption in the present study (Table 3). This is the first study using *A. versicolor* fungus for lithium(I) biosorption and its high efficiency seem to be promising for future applications. In addition, it was clearly seen that isolation of *K. marxianus* yeast strain from salty food waste media affected its lithium(I) sorption capacity in a positive way. There are studies in the literature showing that nutrients and ions found in the growth media of the microbial cells effect their cell wall structures and thus biosorption capacities (Simmons & Singleton 1996; Bzducha-Wróbel *et al.* 2012; Zimkus *et al.* 2013). As an example, Bzducha-Wróbel *et al.* (2012) expressed that Mg^{2+} ion addition to

Table 3 | Comparison of lithium(I) biosorption capacities obtained in this study with the values reported in literature

Biosorbent	Uptake capacity (μmol Li/g sorbent)	pH	Initial Li^+ concentration (mg/L)	Biomass concentration (g/L)	Reference
Streptomyces olivaceus HUT6061	73.9	5.8	0.5	0.2	Tsuruta (2005)
Penicillium chrysogenum IAM7106	7.1				
Aspergillus niger AHU7120	0.7				
Arthrobacter nicotianae IAM12342	125.8				
Saccharomyces uvarumia AHU3978	15.6				
Kluyveromyces marxianus IAM4985	3.9				
Biofilm	85.3	7	139	1	Kurniawan & Yamamoto (2015)
Biomass-based hybrid adsorbent	102.7	10	10	2	Günan Yücel & Aksu (2019)
Biomass-based hybrid adsorbent	245.3	10	50	2	Günan Yücel & Aksu (2019)
Aspergillus versicolor	347.9	9	20	1	Present study
Kluyveromyces marxianus	409.2	9	20	1	Present study

the growth media of the *Saccharomyces cerevisiae* and *Candida utilis* yeast strains caused change in their cell wall compositions and improved their Mg^{2+} sorption capacities (Bzducha-Wróbel *et al.* 2012). Another study by Simmons & Singleton (1996) indicated that L-cysteine supplementation enhanced Ag^+ biosorption capacity of *S. cerevisiae* strain (Simmons & Singleton 1996). In the present study, remarkably high lithium(I) binding capacity of the isolated *K. marxianus* strain with only one step and low cost process is quite advantageous and will be of interest in upcoming studies.

Equilibrium isotherms

The adsorption equilibrium data obtained using the biosorbents were determined to fit both of the applied adsorption equilibrium models in the concentration ranges studied (Figure 4 and Table 4). These results can be associated with the rough and raptured surfaces of the sorbents

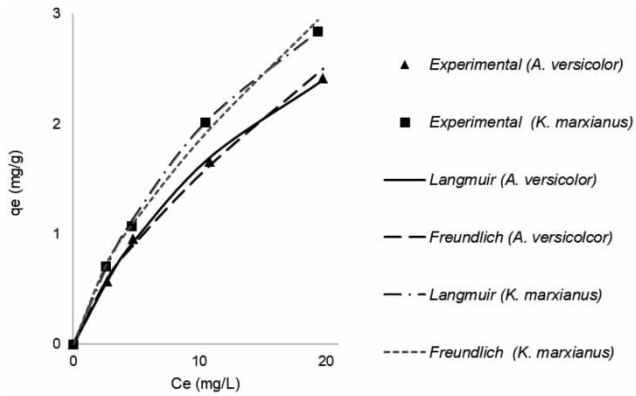

Figure 4 | Langmuir and Freundlich adsorption isotherm models for lithium(I) adsorption onto *A. versicolor* and *K. marxianus*.

Table 4 | Langmuir and Freundlich isotherm constants and coefficients of correlation for lithium(I) adsorption on *A. versicolor* and *K. marxianus*

	Langmuir			Freundlich		
Biosorbent	q_m (mg/g)	K_L (L/mg)	R^2	K_F (mg/g (L/mg)$^{1/n}$)	n_F	R^2
A. versicolor	4.785	0.051	0.993	0.296	1.399	0.992
K. marxianus	5.467	0.056	0.992	0.372	1.432	0.996

including an adequate amount of binding sites for the lithium(I) ions in the solution. However, Langmuir isotherm model is preferred for this case since it provides insight on the maximum capacities of the biosorbents. In Langmuir isotherm model, q_m values of 4.785 mg/g and 5.467 mg/g obtained for biosorption of lithium(I) by *A. versicolor* and *K. marxianus* cells, respectively, demonstrate their higher capacities compared to the one (2.376 mg/g) obtained through the biosorption process on biomass-based hybrid adsorbent (Günan-Yücel & Aksu 2019). In Freundlich isotherm model, greater magnitude of the K_F constant obtained with *K. marxianus* cells revealed with its higher sorption capacity at equilibrium concentration (Negm *et al.* 2018). Besides, n_F values greater than unity confirm that lithium(I) ions were adsorbed favorably onto the both sorbents at the studied conditions (Farooq *et al.* 2010).

CONCLUSIONS

This study shows that lithium(I) ion, which is an important trace element used in various industries, can be captured

from aqueous solutions efficiently and cost effectively by using *A. versicolor* and *K. marxianus* cells. Effects of cell wall structure on their biosorption capacities were evaluated comparatively through FTIR, SEM, surface area and zeta potential analyses. Characterization studies demonstrated that *K. marxianus* cells have higher surface area and negativity, which provide important advantage on its cation sorption properties. Biosorption experiments showed that this is a rapid process occurring in a few minutes. *K. marxianus* strain, which was newly isolated from salty food wastes, showed better performance in all cases studied. Lithium(I) biosorption capacities of the sorbents were determined to be considerably influenced by the parameters of initial pH, initial lithium(I) concentration. Maximum lithium(I) uptake capacities were observed at pH 9 for both biosorbents. Increasing lithium(I) concentration and decreasing cell concentration enhanced lithium(I) adsorbed amount per unit biomass. The equilibrium data obeyed both Langmuir and Freundlich isotherm models at the experimental conditions tested. The impressive performance of *K. marxianus* strain showed that its use in lithium(I) sorption is a considerable alternative since it is an efficient, low cost, eco-friendly and rapid process, and this potential should be evaluated in further studies.

REFERENCES

Aksu, Z. & Dönmez, G. 2000 The use of molasses in copper(II) containing wastewaters: effects on growth and copper(II) bioaccumulation properties of *Kluyveromyces marxianus*. *Process Biochemistry* **36**, 451–458.

Aksu, Z. & Dönmez, G. 2006 Binary biosorption of cadmium(II) and nickel(II) onto dried *Chlorella vulgaris*: Co-ion effect on mono-component isotherm parameters. *Process Biochemistry* **41**, 860–868.

An, J. W., Kang, D. J., Tran, K. T., Kim, M. J., Lim, T. & Tran, T. 2012 Recovery of lithium from Uyuni salar brine. *Hydrometallurgy* **117–118**, 64–70.

Arıca, M. Y., Tüzün, İ., Yalçın, E., İnce, Ö. & Bayramoğlu, G. 2005 Utilisation of native, heat and acid-treated microalgae *Chlamydomonas reinhardtii* preparations for biosorption of Cr(VI) ions. *Process Biochemistry* **40**, 2351–2358.

Bahafid, W., Tahri Joutey, N., Asri, M., Sayel, H., Tirry, N. & El Ghachtouli, N. 2017 *Yeast Biomass: An Alternative for Bioremediation of Heavy Metals Yeast – Industrial Applications*, Antonio Morata and Iris Loira, IntechOpen, London, UK.

Beni, A. A. & Esmaeili, A. 2020 Biosorption, an efficient method for removing heavy metals from industrial effluents: a review. *Environmental Technology & Innovation* **17**, 100503.

Bi, Q., Zhang, Z., Zhao, C. & Tao, Z. 2014 Study on the recovery of lithium from high Mg^{2+}/Li^{+} ratio brine by nanofiltration. *Water Science and Technology* **70**, 1690–1694.

Bodin, H., Mietto, A., Ehde, P. M., Persson, J. & Weisner, S. E. B. 2012 Tracer behaviour and analysis of hydraulics in experimental free water surface wetlands. *Ecological Engineering* **49**, 201–211.

Burattini, E., Cavagna, M., Dell'Anna, R., Malvezzi Campeggi, F., Monti, F., Rossi, F. & Torriani, S. 2008 A FTIR microspectroscopy study of autolysis in cells of the wine yeast *Saccharomyces cerevisiae*. *Vibrational Spectroscopy* **47**, 139–147.

Bzducha-Wróbel, A., Błażejak, S. & Tkacz, K. 2012 Cell wall structure of selected yeast species as a factor of magnesium binding ability. *European Food Research Technology* **235**, 355–366.

Chergui, A., Bakhti, M. Z., Chahboub, A., Haddoum, S., Selatnia, A. & Junter, G. A. 2007 Simultaneous biosorption of Cu^{2+}, Zn^{2+} and Cr^{6+} from aqueous solution by *Streptomyces rimosus* biomass. *Desalination* **206**, 179–184.

Chitrakar, R., Kanoh, H., Miyai, Y. & Ooi, K. 2001 Recovery of lithium from seawater using manganese oxide adsorbent (H1.6mn1.6O4) derived from Li1.6mn1.6O4. *Industrial & Engineering Chemistry Research* **40**, 2054–2058.

Crini, G., Peindy, H. N., Gimbert, F. & Robert, C. 2007 Removal of C.I. Basic Green 4 (Malachite Green) from aqueous solutions by adsorption using cyclodextrin-based adsorbent: kinetic and equilibrium studies. *Separation and Purification Technology* **53**, 97–110.

Farooq, U., Kozinski, J. A., Khan, M. A. & Athar, M. 2010 Biosorption of heavy metal ions using wheat based biosorbents – a review of the recent literature. *Bioresource Technology* **101**, 5043–5053.

Garip, S., Gozen, A. C. & Severcan, F. 2009 Use of Fourier transform infrared spectroscopy for rapid comparative analysis of *Bacillus* and *Micrococcus* isolates. *Food Chemistry* **113** (4), 1301–1307.

Gohari, M., Hosseini, S. N., Sharifnia, S. & Khatami, M. 2013 Enhancement of metal ion adsorption capacity of *Saccharomyces cerevisiae*'s cells by using disruption method. *Journal of Taiwan Institute of Chemistry Engineers* **44**, 637–645.

Günan-Yücel, H. & Aksu, Z. 2019 Enhancing lithium ion capture by using a negatively overcharged biomass-based hybrid adsorbent. *Journal of Environmental Chemistry Engineering* **7**, 103337.

Headley, T. R., Herity, F. & Davison, L. 2005 Treatment at different depths and vertical mixing within a 1-m deep horizontal subsurface-flow wetland. *Ecological Engineering* **25**, 567–582.

Hui, X., Geng, L., Cheng-Bing, Y. & Chong, L. 2016 Effects of the functional group on the lithium ions across the port of carbon nanotube. *Journal of Computational and Theoretical Nanoscience* **13**, 4687–4693.

Jeppson, D. W., Ballif, J. L., Yuan, W. W. & Chou, B. E. 1978 *Lithium Literature Review: Lithium's Properties and*

Interactions. Hanford Engineering Development Laboratory, Richland, WA, USA.

Kim, S., Lee, J., Kang, J. S., Jo, K., Kim, S., Sung, Y. E. & Yoon, J. 2015 Lithium recovery from brine using a lambda-MnO_2/activated carbon hybrid supercapacitor system. *Chemosphere* **125**, 50–56.

Kuligowski, J., Quintás, G., Herwig, C. & Lendl, B. 2012 A rapid method for the differentiation of yeast cells grown under carbon and nitrogen-limited conditions by means of partial least squares discriminant analysis employing infrared micro-spectroscopic data of entire yeast cells. *Talanta* **99** (Supplement C), 566–573.

Kurniawan, A. & Yamamoto, T. 2015 Biosorption of lithium using biofilm matrix of natural microbial consortium. *Microbiology Indonesia* **9**, 106–112.

Mähler, J. & Persson, I. 2012 A study of the hydration of the alkali metal ions in aqueous solution. *Inorganic Chemistry* **28** (1), 425–438.

Mameri, N., Boudries, N., Addour, L., Belhocine, D., Lounici, H., Grib, H. & Pauss, A. 1999 Batch zinc biosorption by a bacterial nonliving *Streptomyces rimosus* biomass. *Water Research* **33**, 1347–1354.

Nath, J. & Ray, L. 2015 Biosorption of Malachite green from aqueous solution by dry cells of *Bacillus cereus* m116 (MTCC 5521). *Journal of Environmental Chemical Engineering* **3**, 386–394.

Negm, N. A., Abd El Wahed, M. G., Hassan, A. R. A. & Abou Kana, M. T. H. 2018 Feasibility of metal adsorption using brown algae and fungi: effect of biosorbents structure on adsorption isotherm and kinetics. *Journal of Molecular Liquids* **264**, 292–305.

Park, J., Sato, H., Nishihama, S. & Yoshizuka, K. 2012 Separation and recovery of lithium from geothermal water by sequential adsorption process with λ-MnO_2 and TiO_2. *Ion Exchange Letters* **5**, 1–5.

Peiro, L. T., Villalba, G. & Ayres, R. U. 2013 Lithium: Sources, Production, Uses, and Recovery Outlook. *The Journal of the Minerals, Metals & Materials Society* **65**, 986–996.

Potocki, L., Depciuch, J., Kuna, E., Worek, M., Lewinska, A. & Wnuk, M. 2019 FTIR and Raman spectroscopy-based biochemical profiling reflects genomic diversity of clinical candida isolates that may be useful for diagnosis and targeted therapy of candidiasis. *International Journal of Molecular Sciences* **20**, 988.

Pradhan, D., Sukla, L. B., Mishra, B. B. & Devi, N. 2019 Biosorption for removal of hexavalent chromium using microalgae *Scenedesmus* sp. *Journal of Cleaner Production* **209**, 617–629.

Sahmoune, M. N. 2018 Performance of *Streptomyces rimosus* biomass in biosorption of heavy metals from aqueous solutions. *Microchemical Journal* **141**, 87–95.

Sahmoune, M. N., Louhab, K. & Boukhiar, A. 2009 Biosorption of Cr (III) from aqueous solutions using bacterium biomass *Streptomyces rimosus*. *International Journal of Environmental Research* **3**, 229–238.

Selatnia, A., Bakhti, M. Z., Madani, A., Kertous, L. & Mansouri, Y. 2004 Biosorption of Cd^{2+} from aqueous solution by a NaOH-treated bacterial dead *Streptomyces rimosus* biomass. *Hydrometallurgy* **75**, 11–24.

Shapaval, V., Afseth, N. K., Vogt, G. & Kohler, A. 2014 Fourier transform infrared spectroscopy for the prediction of fatty acid profiles in *Mucor* fungi grown in media with different carbon sources. *Microbial Cell Factories* **13**, 86.

Simmons, P. & Singleton, I. 1996 A method to increase silver biosorption by an industrial strain of *Saccharomyces cerevisiae*. *Applied Microbiology and Biotechnology* **45**, 278–285.

Taştan, B. E., Ertuğrul, S. & Dönmez, G. 2010 Effective bioremoval of reactive dye and heavy metals by *Aspergillus versicolor*. *Bioresource Technology* **101**, 870–876.

Tsuruta, T. 2005 Removal and recovery of lithium using various microorganisms. *Journal of Bioscience and Bioengineering* **100**, 562–566.

Wang, J. & Chen, C. 2009 Biosorbents for heavy metals removal and their future. *Biotechnology Advances* **27** (2), 195–226.

Zimkus, A., Misiūnas, A. & Chaustova, L. 2013 Lithium(I) effect on the cell wall of the yeast *Saccharomyces cerevisiae* as probed by FT-IR spectroscopy. *Central European Journal of Biology* **8**, 724–729.

First received 4 December 2019; accepted in revised form 10 March 2020. Available online 23 March 2020